Ontogenetic, dietary, and environmental shifts in Mesosauridae

Antoine Verrière[1], Jörg Fröbisch[1,2]

[1] Museum für Naturkunde, Leibniz-Institut für Evolutions- und Biodiversitätsforschung, Invalidenstraße 43, 10115 Berlin, Germany
[2] Institut für Biologie, Humboldt-Universität zu Berlin, Unter den Linden 6, 10099 Berlin, Germany

Corresponding Author:
Antoine Verrière[1]
Museum für Naturkunde, Leibniz-Institut für Evolutions- und Biodiversitätsforschung,
Invalidenstraße 43, 10115 Berlin, Germany
Email address: antoine.verriere@mfn.berlin

Abstract

Mesosaurs are the first secondarily aquatic amniotes and one of the most enigmatic clades of reptiles from the early Permian. They have long puzzled paleontologists with their unique morphologies: possessing an elongated skull with thin needle-like teeth, a long neck, large webbed hindlimbs, banana-shaped pachyosteosclerotic ribs, and a long tail. Here, we look at a large dataset of morphometric measurements from 270 mesosaur specimens in collections around the world. These measurements characterize skull, tooth, and limb proportions and their variation with size. This data presents evidence of surprising ontogenetic changes in these animals as well as new insights into their taxonomy. Our results support the recent hypothesis that *Mesosaurus tenuidens* is the only valid species within Mesosauridae and suggest that "*Stereosternum tumidum*" and "*Brazilosaurus sanpauloensis*" represent immature stages or incomplete specimens of *Mesosaurus* by showing that all three species occupy an incomplete portion of the overall size range of mesosaurs. Under the single-species hypothesis, we highlight a number of ontogenetic trends: (1) a reduction in skull length accompanied by an elongation of the snout within the skull, (2) an elongation of teeth, (3) a reduction in hind limb length, and (4) a reduction in manus length. Concurrent with these changes, we hypothesize that mesosaurs went through a progressive ecological shift during their growth, with juveniles being more common in shallow water deposits, whereas large adults are more frequent in pelagic sediments. These parallel changes suggest that mesosaurs underwent a diet and lifestyle transition during ontogeny, from an active predatory lifestyle as juveniles to a more filter-feeding diet as adults. We propose that this change in lifestyle and environments may have been driven by the pursuit of different food sources, but a better understanding of the Irati Sea fauna will be necessary to obtain a more definitive answer to the question of young mesosaur diet.

Introduction

Mesosaurs are small marine parareptiles from the early Permian and one of the most enigmatic clades of early amniotes. Although they are exclusively found in the deposits of what was at the time a hypersaline inland sea extending over today's eastern South America and southern Africa (Oelofsen & Araújo, 1983; Piñeiro et al., 2012b; Matos et al., 2017; Bastos et al., 2021), and despite their short period of existence (Soares, 2003), mesosaurs represent a key snapshot in amniote evolutionary history. Indeed, they are the first secondarily aquatic amniotes, i.e., the first fully terrestrial tetrapods to have return to live in water (Carroll, 1988). Yet their affinities are controversial, their origins are poorly known, and their lineage ended with them (Laurin & Piñeiro, 2017; MacDougall et al., 2018; Ford & Benson, 2020). Until recently, three monotypic genera were recognized: *Mesosaurus tenuidens* (Gervais, 1869), "*Stereosternum tumidum*" (Cope, 1886), and "*Brazilosaurus sanpauloensis*" (Shikama & Ozaki, 1966). Although these three taxa were originally supported by a number of diagnostic characters (Shikama & Ozaki, 1966; Araújo, 1976; Oelofsen & Araújo, 1987; Modesto, 1999, 2006, 2010), a recent review (Piñeiro et al., 2021) deemed these characters arbitrary and suggested *Mesosaurus*

55 *tenuidens* to be the only valid species with "*Brazilosaurus*" and "*Stereosternum*" representing
56 junior synonyms of *Mesosaurus*.
57   All mesosaurs present a striking morphology: a slender body with a very long tail, paddle-like
58 hind limbs, a massive ribcage with thickened banana-shaped ribs, an elongated neck holding an
59 elongate but very thin skull, and a long snout bearing thin needle-like teeth (Fig. 1). This peculiar
60 appearance has resulted in conflicting hypotheses about their ecology, from amphibious (Núñez
61 Demarco et al., 2018) to fully marine (Modesto, 1999, 2010; Canoville & Laurin, 2010), from
62 undulatory (Braun & Reif, 1985; Villamil et al., 2015) to partially limb-propelled swimmers (da
63 Silva & Sedor, 2017; MacDougall et al., 2020).
64   More than other aspects of their anatomy, the long thin teeth of mesosaurs have puzzled those
65 who studied them the most. If they are somewhat reminiscent of those of other vertebrates such
66 as dolphins or gharials, mesosaur teeth are singular in their length and their needle-like
67 morphology. Consequently, they have no modern analog, which has led to contradicting attempts
68 at characterizing the feeding habits of mesosaurs. Based on cranial morphology alone,
69 MacGregor (1908) proposed a "fish"-based diet for mesosaurs. Subsequent studies discarded this
70 interpretation (Wiman, 1925; Araújo, 1976), noting that their teeth were too fragile for active
71 hunting and pointing to the absence of "fish" in mesosaur-bearing strata (Oelofsen & Araújo,
72 1983; Piñeiro et al., 2012b), although recent works show that fish were more frequent than
73 previously thought (Xavier et al., 2018). In fact, based on their tooth morphology (Pretto,
74 Cabreira & Schultz, 2012), the fauna of the Irati-Whitehill Sea (Piñeiro et al., 2012b; Chahud &
75 Petri, 2013; Xavier et al., 2018), as well as gut content and coprolite analyses (Silva et al., 2017),
76 most authors concluded that mesosaurs were filter-feeders trapping pygocephalomorph
77 crustaceans in the net of their teeth (Oelofsen & Araújo, 1983; Modesto, 1999, 2006, 2010;
78 Piñeiro et al., 2012b; Silva et al., 2017). Despite this, some authors suggested that mesosaurs
79 could have been active hunters (Pretto, Cabreira & Schultz, 2012) or even scavengers (Silva et
80 al., 2017).
81   Although interest and research effort into the paleobiology of mesosaurs has tremendously
82 increased in the last decade and some aspects of mesosaur ecology have been addressed in the
83 past, their lifestyle throughout ontogeny has not been fully investigated. Even though some
84 authors have looked at the morphometrics of mesosaurs (Araújo, 1976; Rossmann & Maisch,
85 1999; Rossmann, 2000, 2002; Núñez Demarco et al., 2018; Piñeiro et al., 2021) or at histological
86 growth marks (de Ricqlès, 1974; Canoville & Laurin, 2010; Klein et al., 2019), there have only
87 been a few studies focusing on their ontogeny (Piñeiro et al., 2012a; Piñeiro, Núñez Demarco &
88 Meneghel, 2016; Núñez Demarco et al., 2018; Bickelmann & Tsuji, 2018; Verrière, Fröbisch &
89 Fröbisch, 2021; Núñez Demarco, Ferigolo & Piñeiro, 2022). This is surprising, as mesosaurs
90 constitute a unique framework for understanding the complex links between diet and
91 morphology in the fossil record. First, they comprise one of the few comprehensive ontogenetic
92 series known in fossil amniotes (Piñeiro et al., 2012a; Piñeiro, Núñez Demarco & Meneghel,
93 2016; Bickelmann & Tsuji, 2018; Núñez Demarco, Ferigolo & Piñeiro, 2022). Second, they
94 lived in a constrained environment with greatly reduced food variety, placing considerable limits

95   on what their feeding habits could have been (Soares, 2003; Piñeiro et al., 2012b; Xavier et al.,
96   2018). Lastly, they are the first secondarily aquatic amniotes, and understanding their dietary
97   evolution has implications for the reconstruction of feeding habits in later marine amniotes.
98   Here, we provide the first quantitative assessment of ontogenetic changes in mesosaurs on
99   such a large number of specimens. With this dataset, we test the hypothesis from Núñez
100 Demarco et al. (2022) that mesosaur grow isometrically. Our results support the single-species
101 model of Piñeiro et al. (2021) by demonstrating that the formerly recognized species occupy
102 incomplete segments of the mesosaur size range and show very little difference between them.
103 Based on the single-species model, we do not retrieve the isometric growth measured by Núñez
104 Demarco et al. (2022) and instead show that the ontogeny of mesosaurs is marked by some
105 significant allometric transformations and environmental partitioning, likely indicating a change
106 in diet and lifestyle with growth.
107

Materials & Methods
108
Material investigated
109
110   We examined 270 articulated mesosaur specimens from collections around the world. Of
111 these, 115 were previously attributed to *Mesosaurus tenuide*ns, 96 to "*Stereosternum tumidum*",
112 13 to "*Brazilosaurus sanpauloensis*", and 46 were unidentified (Supp. Table 1). Of the identified
113 specimens, 47 had a preserved skull and teeth, with 18 attributed to *Mesosaurus*, 29 to
114 "*Stereosternum*", and only one to "*Brazilosaurus*". Earlier studies mentioned the presence of
115 teeth in "*Brazilosaurus*" (Rossmann, 2002; Modesto, 2006; Silva et al., 2017), all of them
116 relying on the average tooth length of 2 mm provided by Rossmann (2002). We find this value
117 contentious in different regards. First, Rossmann (2002) did not provide the raw measurements
118 for his calculation. Second, we reexamined the material described by Rossmann (2000, 2002) as
119 bearing teeth and noticed that elements he describes as teeth are in fact misidentified broken
120 tooth sockets from the maxilla or the dentary (Supp. Fig. 1). Finally, out of the twelve specimens
121 assigned to "*Brazilosaurus*" studied here, only ROM 28496 had some visible complete teeth. In
122 all other specimens, teeth are either missing or completely broken, in any case not in a state of
123 preservation allowing their measurement. Consequently, we must dismiss the average tooth
124 length for "*Brazilosaurus*" of 2 mm given by Rossmann (2002). For this reason, no specimens
125 previously attributed to "*Brazilosaurus*" are included in our statistical analysis of teeth.
126

Measurements
127
128   For each specimen, we measured the length of most preserved long bones: humerus, radius,
129 ulna and metacarpals in the forelimb; femur, tibia, fibula, and metatarsals in the hind limbs.
130 When possible, we also measured autopod length, from the proximal edge of the intermedium to
131 the distal tip of digit III for the forelimb, and from the proximal edge of the astragalus to the
132 distal tip of digit V in the hind limb, as digit III and V are the longest digits in the anterior and
133 posterior autopod, respectively. In juveniles where carpals and tarsals were not ossified, the
134 distalmost portions of the ulna or fibula were taken as most proximal extent of the autopodium.

135   To account for cranial proportions, we measured the total skull length as well as antorbital and
136   postorbital length.
137   Likely due to dental replacement, mesosaur teeth can greatly vary in size within a single
138   specimen (Modesto, 1999, 2006; Piñeiro et al., 2021). To better account for the dimensions of
139   mesosaur teeth, we therefore chose not to use average tooth length and diameter, unlike previous
140   works (Piñeiro et al., 2021). Instead, we measured the length of the longest visible tooth and the
141   diameter of this tooth at its base.
142   Our specimens were preserved in various states of completeness, with some showing only the
143   anterior or the posterior half of the body and others missing limbs or neck while others were
144   mostly complete. Unlike Núñez Demarco et al. (2022) who studied ontogenetic variation within
145   bones, we wanted a shared proxy for specimen size to be able to model and compare variations
146   in all bones independently. Thus, we calculated the average centrum length of dorsal vertebrae
147   for each specimen, as this measurement has been shown to be a reliable estimate for body length
148   (Núñez Demarco et al., 2018).
149   All measurements were taken using a caliper directly on specimens or Fiji 1.53c on distortion-
150   corrected high-resolution photographs.
151
152   Facies
153   Mesosaur specimens can be found in various deposits that represent different sections of the
154   carbonate ramp boarding the Irati-Whitehill Sea (Xavier et al., 2018; Ng, Vega & Maranhão,
155   2019). To account for size distribution across deposit environments and potential niche
156   partitioning of ontogenetic stages in mesosaurs, we categorized our specimens into five facies: (i)
157   yellow limestone, (ii) white calcarenite, (iii) grey siltstone, (iv) grey mudstone, and (v)
158   bituminous black shales. These facies represent a gradient in depth, energy level, and
159   oxygenation of the water layers.
160
161   Statistics
162   According to Huxley (1932), simple allometry is described by the equation
163    $y = kx^{\alpha}$ or in its logarithmic form
164    $\log y = \alpha \log x + \log k$
165   The allometric coefficient α characterizes the slope of the linear relationship between the logged
166   valued of y and x and $\log k$ is the intercept of the linear relationship. Thus, an isometric growth
167   (no changes in proportion to size during ontogeny) is characterized by an allometry coefficient of
168    $\alpha = 1$ while values of $\alpha > 1$ and $\alpha < 1$ respectively reflect positive and negative allometry.
169   By transforming the simple allometry equation to express the ratio y/x rather than y as a
170   function of x, we obtain
171    $\dfrac{y}{x} = kx^{\alpha - 1}$ which in turns gives

172    $\log \dfrac{y}{x} = (\alpha - 1) \log x + \log k$

173   In this equation we can define another allometry coefficient $\beta = \alpha - 1$. Thus, for the same values
174   of x and y, isometry is defined by $\beta = 0$ while negative and positive allometry are respectively
175   characterized by negative and positive values of β, improving readability both graphically and
176   numerically (Klingenberg, 1998). Therefore, we prefer β to α in the present study.
177   For each metric, we computed a linear regression model of the logged ratio of the metric's
178   values over size proxy value ($\log \frac{y}{x}$) as a function of logged size proxy values ($\log x$) and
179   calculated the allometry coefficient β to test for proportion changes throughout ontogeny.
180   Similarity between species was also tested for each measurement. Linear modelling and
181   statistical analyses were carried out in R 4.0.5 (R. Core Team, 2021).
182

Results
184   Three-species hypothesis
185   *Skull*
186   Skull measurements behave differently with respect to size in the three formerly recognized
187   mesosaur "species". In "*Brazilosaurus*", all three skull measurements show negative allometry,
188   albeit not significant (Table 1). In *Mesosaurus*, postorbital length is the only skull metric to
189   display a significant negative allometry, while total length and antorbital length both show a non-
190   significant positive allometry (Table 1). In "*Stereosternum*", all three skull measurements show
191   significant negative allometry but each with different allometry coefficients (Fig. 2). The
192   negative allometry is less marked for antorbital length ($\beta = -0.090$, p $= 0.022$) than for total
193   length ($\beta = -0.204$, p < 0.001), itself less marked than postorbital length ($\beta = -0.341$, p < 0.001).
194   For all three species, skull measurements rank similarly in terms of allometry coefficients
195   with antorbital length having the highest, followed by total length and finally postorbital length
196   last. This shows how skull elements vary differently in proportion throughout ontogeny. To
197   better account for these variations, we measured the effect of allometry in function of total skull
198   length instead of body size. In this configuration, we obtain very concordant results between the
199   three species: antorbital length shows significant positive allometry, whereas postorbital length
200   shows significant negative allometry (Table 2). Thus, over the course of ontogeny, the
201   postorbital length decreases while the snout increases relative to overall skull length (Fig. 3).
202

203   *Teeth*
204   Several authors have noted an apparent change in tooth morphology between mesosaur
205   species: "*Brazilosaurus*" and "*Stereosternum*" are described as bearing short, straight conical
206   teeth whereas *Mesosaurus* is defined by thin, curved, and elongated teeth (Oelofsen & Araújo,
207   1987; Rossmann, 2002; Modesto, 2006). Indeed, for the same body size, adult *Mesosaurus* teeth
208   are systematically longer than those of "*Stereosternum*" albeit similar in diameter (Fig. 2, 3).
209   Tooth length and diameter in *Mesosaurus* both display positive allometry, although the linear
210   relationship is not significant (Table 1). In "*Stereosternum*", both measurements show a
211   significant negative allometry, with tooth diameter showing the lowest coefficient ($\beta = -0.622$, p
212   < 0.001).

213   Since our results highlight variation in cranial dimensions throughout ontogeny, we also
214   calculated allometry coefficients for tooth measurements with respect to skull length. Surprising,
215   this shows non-significant negative allometry for tooth length in both species, whereas tooth
216   diameter exhibits negative allometry for both species, although it is only significant in
217   "*Stereosternum*" (Table 2). Thus, mesosaur teeth grow in length at the same rate as the skull,
218   meaning that they do not become proportionally longer throughout ontogeny. However, these
219   teeth keep their juvenile diameter and grow only in length in "*Stereosternum*" whereas both
220   length and diameter grow isometrically to the skull in *Mesosaurus* (Fig. 4).
221
222   *Limbs*
223   In all three species, most long bones show no significant difference in growth with isometry
224   (Table 3A-C), meaning that their proportional length with respect to body size does not change
225   throughout ontogeny. However, there are several exceptions to this.
226   In "*Brazilosaurus*", femur, tibia and metatarsal V length show significant negative allometry
227   (Table 3A). Although this might reflect a size reduction of the posterior limb during ontogeny in
228   this species, those measurements are only documented for eight adult specimens in our dataset
229   and likely do not reflect the entire ontogenetic trajectory of the species.
230   In *Mesosaurus*, most forelimb bones exhibit a significant positive allometry, aside from
231   metacarpals II, IV, and V (Fig. 2). While this suggests that the anterior autopod increases in size,
232   there are very few juveniles or subadult *Mesosaurus* in our dataset. Thus, much like for
233   "*Brazilosaurus*", *Mesosaurus* forelimb measurements are concentrated in the adult region of the
234   morphospace, and do not satisfyingly account for the entire ontogenetic variation.
235   In "*Stereosternum*", metacarpal I and metatarsal I also display a significant positive allometry,
236   but femur, tibia, fibula and metacarpal V show a significant negative allometry (Fig. 2).
237   Uniquely in mesosaur "species", the posterior autopod also shows a slight significant negative
238   allometry. This reflects a reduction in limb size with respect to the body. "*Stereosternum*" being
239   the best-documented taxon here, these results are more representative than for the two other
240   species.
241
242   *ANOVAs*
243   We measure a significant effect of species on allometry coefficients for eight measurements:
244   total skull length, antorbital length, postorbital length, tooth length, humerus, femur, tibia, and
245   fibula length (Table 4). However, rather than indicating a real difference between the species,
246   this likely reflects a sampling bias. In the near absence of *Mesosaurus* and "*Brazilosaurus*"
247   juveniles in our dataset, values for these species form clusters concentrated in the adult–size
248   region, which distorts linear regressions (Fig. 2). Therefore, these regressions do not fully
249   account for the ontogenetic trajectories of the measurements.
250
251   Single-species hypothesis
252   In a recent study, Piñeiro et al. (2021) proposed *Mesosaurus tenuidens* to be the only valid
253   species within the clade by statistically rejecting most characters used to discriminate between

254   the three previously recognized mesosaur species. To account for this new hypothesis, we
255   reproduced our analysis with all specimens (re)assigned to *Mesosaurus*.
256
257   *Skull*
258   All three skull measurements show negative allometry when compared to body size, but the
259   linear relationship is only significant for postorbital length and total skull length (Table 1). When
260   measuring allometry with respect to total skull length, the signal is unambiguous, with antorbital
261   length showing positive allometry and postorbital length negative allometry (Fig. 3). Similar to
262   the three-species hypothesis, our results with one species point to an elongation of the snout
263   elongates and a reduction of postorbital length, while overall skull length proportionally
264   decreases with respect to the body.
265   These results differ from those of Núñez Demarco et al. (2022) who measured an isometric
266   relationship of antorbital and postorbital length to total skull length. However, this can be easily
267   explained by a difference in the statistical power of our datasets. We use a much larger dataset
268   (84 specimens vs. 19), including more juveniles and larger specimens, which refines the results
269   by producing smaller confidence intervals. It is therefore likely that the isometry in skull
270   proportion measured by Núñez Demarco et al. (2022) is a statistical artifact caused by the size of
271   their dataset.
272
273   *Teeth*
274   Under the single-species hypothesis, tooth length shows positive but non-significant allometry
275   whereas diameter shows a significant negative allometry with respect to body size. However,
276   when compared to skull size, tooth length exhibits a strong significant positive allometry and
277   tooth diameter a significant negative allometry (Table 2). In practice, tooth diameter remains the
278   same in adults as in juveniles, but teeth elongate throughout ontogeny and become more needle-
279   like.
280
281   *Limbs*
282   There is a strong trend to hind limb reduction when considering a single mesosaur taxon (Fig.
283   5). All eight long bone measurements display negative allometry coefficients in relation to body
284   size and this relationship is significant for seven of them (Table 3D). Only metatarsal I length is
285   not significantly isometric in growth. Posterior autopod length also shows a significant negative
286   allometry.
287   In contrast, forelimb long bones do not show such a reduction in size. Only metacarpals
288   display significant negative allometry, with the exception of metacarpal I that has a non-
289   significant positive allometry coefficient. Thus, while stylopod and zeugopod do not vary in
290   proportions, it appears the manus is reduced during ontogeny.
291   At first glance, it could seem that these results do not match those of Núñez Demarco et al.
292   (2022), who report isometric growth in mesosaur limbs. Nevertheless, our findings are
293   compatible with theirs. What Núñez Demarco et al. (2022) measure is that long bones grow
294   isometrically with respect to their respective stylopod, humerus length for fore limbs and femur

295   for hind limbs. What we measure is the allometry of these bones with respect to size. Here we
296   show that femur length displays a significant negative allometry with respect to size, and so do
297   most other limb bones. In sum, the isometric growth measured by Núñez Demarco et al. (2022),
298   and by extension their other results for limbs, is likely an effect of using different reference
299   frames.
300
301   Environmental distribution
302   Figure 6 shows the distribution of size classes in the main facies of the Irati-Whitehill Sea. In
303   our sample, small mesosaurs (i.e., juveniles) are overrepresented in limestone, although they also
304   occur in siltstone and black shales. Mid-sized mesosaurs are well represented in all facies despite
305   frequency variations due to sample size differences. Contrary to what has been hypothesized
306   (Núñez Demarco et al., 2018), we do not find that large specimens are only found in the marginal
307   regions of the basin. Instead, in our dataset, very large specimens (vertebral length $\geq$ 10 mm) are
308   exclusively found in mudstone and black shales, facies that correspond to deeper, more pelagic,
309   and more anoxic environments (Xavier et al., 2018; Bastos et al., 2021).
310

311   **Discussion**
312   Missing juveniles and single-species hypothesis
313   One of the most significant results of our study is not found with regards to size and
314   proportional changes in mesosaur anatomy but instead in the distribution of body size itself.
315   Despite the 270 specimens examined here, there are a number of surprising gaps in the size range
316   covered by our sample (Fig. 7). First, the few "*Brazilosaurus*" specimens studied here are
317   concentrated in the adult size range of "*Stereosternum*", but no juveniles or subadults are
318   preserved. Second, there is a clear divide between the youngest "*Stereosternum*" specimens on
319   the one hand and subadults and adults of that species on the other hand. Third, and more
320   importantly, only two specimens of *Mesosaurus* are the size of juvenile "*Stereosternum*",
321   whereas all other specimens range from the size of "*Stereosternum*" subadults to larger sizes than
322   the largest "*Stereosternum*" specimens. These gaps in size distribution have a direct effect on the
323   interpretation of allometric measurements as they alter the results of linear regressions, making
324   them less representative of ontogenetic changes.
325   Piñeiro et al. (2021) highlighted that most features employed to define mesosaur species are
326   not statistically supported or are practically unusable for identification. Characters like the shape
327   of the interclavicle, tooth length, or presacral vertebral count are highly preservation-dependent,
328   whereas others such as the degree of pachyostosis of ribs or the skull-neck length ratio are
329   subjective and ontogenetically variable (for pachyostosis, see also Klein et al., 2019). This lack
330   of reliable characters led the authors to suggest that both "*Stereosternum tumidum*" and
331   "*Brazilosaurus sanpauloensis*" are junior synonyms of *Mesosaurus tenuidens*.
332   The ontogenetic variability of supposedly taxonomic characters led to an age partitioning of
333   mesosaur specimens into the different "species". On the one hand, juvenile and subadult
334   specimens tended to be identified as "*Stereosternum*", because they bear shorter conical teeth

335   and are usually preserved complete, displaying the maximum number of presacral vertebrae.
336   Both features were formally admitted as prominent characters for mesosaur identification.
337   On the other hand, the largest mesosaur specimens bear longer, thinner teeth and have more
338   markedly pachyostotic ribs, and they tended historically to be attributed to *Mesosaurus*. As for
339   "*Brazilosaurus*" specimens, they were usually identified on the basis of their cervical vertebral
340   count, which is however a misidentification as the result of a displaced rib cage (pers. obs.). In
341   fact, even the original description of the species (Shikama & Ozaki, 1966) miscounted the
342   number of cervicals due to the posterior displacement of dorsal ribs (pers. obs.), which led to the
343   erroneous erection of this feature as a defining character. To summarize, there are several
344   reasons as to why mesosaur invalidated "species" occupy different regions of the size range.
345   Rather than a sampling bias, the size distribution gaps in our dataset more likely reflect a
346   species-identification bias. Our data shows consequent overlap in the morphometrics of all three
347   species. "*Brazilosaurus*" is virtually indistinguishable from "*Stereosternum*", whereas the old
348   definition of *Mesosaurus* seems to have mostly representatives on the higher side of the size
349   spectrum (Fig. 7). Furthermore, the low significance of allometry coefficients (Tables 1, 2, 3) is
350   also likely an effect of the small number of juveniles of the *Mesosaurus* type in our dataset,
351   although more juvenile specimens have been described that we could not include (Piñeiro et al.,
352   2012a).
353   Our results therefore corroborates the single-species hypothesis of Piñeiro et al. (2021) and
354   their discarding of the former characters as ontogenetically variable. In fact, the three previously
355   identified "species" more probably represented three artificial types: the "*Brazilosaurus*"-type is
356   a poorly preserved mesosaur with displaced ribs, the "*Stereosternum*"-type is a size class
357   encompassing juveniles to young adults, and the "*Mesosaurus*"-type represents adults with more
358   extreme sizes and morphologies. Consequently, hereafter we will only consider our results in the
359   light of the single-species hypothesis.
360
361   Environmental partitioning
362   Even when considering *Mesosaurus* as the only valid mesosaur taxon, one puzzling difference
363   between the previously distinct types cannot be explained as an effect of ontogenetic changes or
364   dubious characters alone. Some authors pointed out that the three types were not equally
365   distributed across the facies of the Irati-Whitehill Sea. Oelofsen & Araújo (1983) and Rossmann
366   (2002) noted that "*Brazilosaurus*" and "*Stereosternum*" were more commonly found in
367   limestone deposits, whereas *Mesosaurus* was more frequent in oily black shales. Since these
368   publications however, mesosaur specimens have been described in other facies and the former
369   species have been synonymized, meaning their observations must be considered with caution.
370   Nevertheless, our study demonstrate that size classes are not homogeneously distributed
371   across lithological facies: juveniles are overrepresented in limestone, and very large/old
372   specimens in black shales (Fig. 6). As argued above, flaws in the formerly admitted diagnostic
373   characters have led to juveniles and young adults being preferentially assigned to
374   "*Stereosternum*" and old adults to *Mesosaurus* (Fig. 7). Because we look at articulated

375 specimens, it is also fair to assume that the specimens were buried relatively close to their life
376 environment. Therefore, what Oelofsen & Araújo (1983) and Rossmann (2002) noticed were
377 likely the signs of ontogenetic stage partitioning rather than species partitioning.
378   The overrepresentation of juveniles and large adult in some facies suggests that mesosaurs
379 preferentially occupied some environments at different stages of their life. Juveniles were mostly
380 present in the shallower, more coastal sections of the carbonate ramp, while medium-sized
381 mesosaurs were present in all areas, and the largest and oldest individuals were restricted to
382 pelagic and anoxic regions (Fig. 6). Thus, if mesosaurs were not confined to a specific region of
383 their environment, it seems that, overall, they gradually moved away from the coast during their
384 growth.
385   The pelagic migration of mesosaurs with growth raises the question of their reproduction.
386 Associated articulated juveniles and adults, even gravid individuals, have been found in
387 limestone, siltstone, and mudstone (Piñeiro et al., 2012a; Bickelmann & Tsuji, 2018), but the
388 greater frequency of juveniles in limestone suggests that mesosaurs were mostly born near the
389 coast. If they were oviparous like most reptiles, this would have been easily explained by the
390 necessity to lay eggs on land. However, evidence suggests instead that mesosaurs were
391 viviparous, and possibly even cared for their young (Piñeiro et al., 2012a). Mesosaurs could
392 therefore have given birth anywhere in the sea, making the causes of a partitioning less clear. To
393 try to explain this, we must look at our morphometric analyses.
394
395 Ontogenetic changes and diet shifts
396   Our results show that mesosaur growth is marked by several morphological changes: an
397 elongation of the teeth relative to the skull (Fig. 3), an elongation of the snout (Fig. 4), and a
398 reduction of limbs (Fig. 5). Limb reduction throughout ontogeny hints at a difference in
399 locomotory habits between juveniles and adults. Mesosaurs are swimming reptiles, and the
400 degree of involvement of the limbs in locomotion is still debated. Some authors support the idea
401 of mainly tail-driven mesosaurs (Braun & Reif, 1985; Villamil et al., 2015) while others
402 suggested a potentially larger role of limbs in propulsion (da Silva & Sedor, 2017; MacDougall
403 et al., 2020). Yet, the ontogenetic limb reduction we expose seems incompatible with the
404 conception that limbs were crucial for locomotion. Instead, our results provide evidence for a
405 decreasing involvement of limbs in mesosaur swimming and weigh in favor of a tail-driven
406 model of mesosaur swimming throughout their ontogeny.
407   The association of limb reduction with cranial and dental modifications strongly suggest the
408 existence of locomotion and dietary shift in mesosaur. Such shifts are not rare in reptiles but are
409 usually associated with dietary partitioning between juveniles and adults, meaning they exploit
410 different food sources at different stages of their growth (Arthur, Boyle & Limpus, 2008; Gignac
411 & Erickson, 2015; Dick, Schweigert & Maxwell, 2016; Wang et al., 2017). In the case of
412 mesosaurs, a change in diet could explain the environmental migration we observe in size classes
413 (Fig. 6). As mesosaurs grew, they would have shifted from an abundant food source in the
414 coastal environment to another one more prevalent in pelagic regions or other water layers.

415 Preying on different food sources in different water layers would have been a way to avoid
416 competition between ontogenetic stages in a sea where resources were scarce. Different feeding
417 habits would also explain the presence of juveniles in pelagic environments, as young mesosaurs
418 could have been born anywhere in the sea but would have preferentially migrated to the coastal
419 region looking for food. Yet, there remains the question of the alternative food source.
420   Traditionally, mesosaurs are considered filter-feeders that preyed on pygocephalomorph
421 crustaceans, based on stratigraphic occurrences (Oelofsen & Araújo, 1983; Piñeiro et al., 2012b;
422 Xavier et al., 2018; Ng, Vega & Maranhão, 2019) as well as on gastric contents and coprolites
423 (Piñeiro et al., 2012b; Ramos, 2015; Silva et al., 2017). While this applies to adults, it is unclear
424 what the diet of juveniles could have been. Mesosaur-bearing strata of the Irati-Whitehill Sea
425 deposits are rich in mesosaurs and pygocephalomorphs remains but scarce in other types of
426 fossils. Only rare invertebrate traces, bivalves, and paleonisciform fish scales have been
427 described (Oelofsen & Araújo, 1983; Piñeiro et al., 2012b; Matos et al., 2017; Xavier et al.,
428 2018), although recent works have revised the abundance of paleonisciform fishes upwards
429 (Xavier et al., 2018). This raises a puzzling question: if juvenile mesosaurs did not have the same
430 diet as adults, what could they possibly have been eating?
431   Our morphometric analysis shows that young mesosaurs would have had longer limbs, shorter
432 snouts and shorter teeth than adults, a morphology better suited to active hunting than that of
433 adults. Among the known Irati-Whitehill fauna, only pygocephalomorph crustaceans and
434 paleonisciform fishes could have been the subject of active hunting. Thus, juvenile mesosaurs
435 could have actively preyed on small fish or large pygocephalomorphs, while mesosaurs would
436 have slowly filtered waters to catch smaller pygocephalomorphs or even larvae. The coastal
437 environment would have been better oxygenated and richer in nutrients, fostering the growth of
438 larger preys, whereas smaller crustaceans could have occupied the harsher pelagic waters.
439 Unfortunately, the ecology of pygocephalomorph crustaceans or paleonisciform fish is very
440 poorly known. One way of testing this hypothesis would be to examine size distribution across
441 facies for fish and crustaceans and see if there is a trend, similar to what we did for mesosaurs.
442   Another possible answer is that juvenile mesosaurs fed on animals that did not preserve well
443 under the conditions where mesosaurs were buried. High energy conditions in the mid-coastal
444 environments as well as acidic anoxic waters in the black shale environment might have
445 hampered the preservation of some animals. Moreover, young mesosaurs could have eaten
446 jellyfish or soft invertebrates with little to no mineralized tissues, which greatly reduces the
447 chances at fossilizing the latter. Although the sea's hypersaline conditions would not have
448 favored such animals (Piñeiro et al., 2012b; Bastos et al., 2021), there are occurrences of soft
449 invertebrates in hypersaline contexts (Parker, 1959; Tanner, Glenn & Moore, 1999; Gilabert,
450 2001). Yet, there are many cases of outstanding preservation in the Irati-Whitehill sediments
451 producing complete articulated fossils (Modesto, 1999, 2010; Piñeiro et al., 2012b; Núñez
452 Demarco et al., 2018), sometimes even showing soft tissue preservation (Piñeiro et al., 2012b,a;
453 MacDougall et al., 2020). With such conditions of preservation, it seems very unlikely that no
454 trace of other invertebrates would remain. It is possible, however, that soft animal fossils are yet

455 to be discovered, and that further study of the mesosaur-bearing Irati-Whitehill deposits will
456 reveal them.
457

Conclusions

459   After examining a large sample of mesosaur morphometric measurements, we present
460 evidence of ontogenetic changes in these animals as well as insights into their taxonomy. First,
461 our results demonstrate that the three previously identified species occupy incomplete portions of
462 the size range of mesosaurs and show very minor differences in body proportions otherwise. This
463 supports the proposition of Piñeiro et al. (2021) that *Mesosaurus tenuidens* is the only valid
464 species and indicates that "*Stereosternum tumidum*" and "*Brazilosaurus sanpauloensis*" likely
465 represent immature stages or incomplete specimens of *Mesosaurus*.
466   Our results also highlight the following ontogenetic trends:
467 • a reduction in skull length accompanied by an elongation of the snout within the skull
468 • an elongation of teeth
469 • a reduction in hind limb length
470 • a reduction in manus length
471 These ontogenetic trends are associated with a partitioning of ontogenetic stages across facies
472 following a gradient of depth and distance to the coast. This suggests that mesosaurs underwent a
473 diet and lifestyle transition during their growth: juveniles had an active predatory lifestyle in a
474 coastal environment, while old adults adopted a more filter-feeding diet in more pelagic and
475 anoxic waters. Our hypothesis is that mesosaurs exploited different food sources during their
476 lifetime, but further study of the Irati-Whitehill Sea fauna will be necessary to truly test this.
477

Institution Acronyms

479   **AMNH**: American Museum of Natural History, New York, NY, USA. **BSPG**: Bayerische
480 Staatssammlung für Paläontologie und Geologie, Munich, Germany. **CM**: Carnegie Museum of
481 Natural History, Pittsburgh, PA, USA. **IGC**: Instituto Geográfico e Cartográfico do Estado de
482 São Paulo, São Paulo, SP, Brazil. **GPIT**: Geologisch-Palaeontologisches Institut Tübingen,
483 Tübingen, Germany. **MB**: Museum für Naturkunde, Berlin, Germany. **MCZ**: Museum of
484 Comparative Zoology, Cambridge, MA, USA. **MfNM**: Museum für Naturkunde Magdeburg,
485 Magdeburg, Germany. **MNHN**: Muséum National d'Histoire Naturelle, Paris, France. **MZSP**:
486 Museu de Zoologia da USP, São Paulo, SP, Brazil. **NMNS**: National Museum of Nature and
487 Science, Tokyo, Japan. **NHMW**: Naturhistorisches Museum Wien, Vienna, Austria. **NRM**:
488 Naturhistoriska Riksmuseet, Stockholm, Sweden. **PIMUZ**: Paläontologische und Zoologische
489 Museum, Zürich, Switzerland. **ROM**: Royal Ontario Museum, Toronto, ON, Canada. **SMF**:
490 Senckenberg Museum Frankfurt, Frankfurt am Main, Germany. **SMNK**: Staatliches Museum für
491 Naturkunde Karlsruhe, Karlsruhe, Germany. **SMNS**: Staatliches Museum für Naturkunde
492 Stuttgart, Stuttgart, Germany. **UFRGS**: Universidade Federal do Rio Grande do Sul, Porto
493 Alegre, RS, Brazil. **UFSCar**: Universidade Federal de São Carlos, São Carlos, SP, Brazil.

494 **URCR**: Universidade Estadual Paulista, Campus de Rio Claro, Rio Claro, SP, Brazil. **USNM**:
495 National Museum of Natural History, Washington, DC, USA
496

Acknowledgements

498   For granting us access to specimens and for their help and hospitality during our collection
499 visits, we are extremely thankful to Carl M. Mehling (AMNH), Oliver Rauhut (BSPG), Juliana
500 Leme (IGC), Ingmar Werneburg (GPIT), Thomas Schossleitner (MB), Jessica Cundiff (MCZ),
501 Michael Buchwitz (MfNM), Nour-Eddine Jalil (MNHN), Alberto B. Carvalho (MZSP), Ursula
502 Göhlich (NHMW), Thomas Mörs (NRM), Christian Klug (PIMUZ), Kevin Seymour (ROM),
503 Rainer Brocke (SMF), Eberhard Frey (SMNK), Rainer Schoch and Erin Maxwell (SMNS),
504 Cesar Leandro Schulz, Thiago Carlisbino, and Voltaire Paes Neto (UFRGS), Aline Ghilardi, Tito
505 Aureliano, and Marcelo A. Fernandes (UFSCar), Reinaldo Bertini (URCR), and Amanda
506 Millhouse (USNM). Many thanks to Amy Henrici (CM) and Makoto Manabe (NMNS) for
507 providing us with high resolution photographs of the mesosaur specimens in their collections.
508 Thanks to Yara Haridy for her ideas and support that helped spark this project. We would like to
509 thank Esther Ullrich-Lüter for catalyzing the drafting of this manuscript. We are also very
510 thankful to Vanuhi Hambardzumyan and Mark MacDougall for providing very helpful
511 comments at different stages of the manuscript. A. Verrière would like to address very special
512 thanks to Heitor Satorelli for his friendship, for his heartfelt hospitality and for helping him
513 navigate through Brazil. We would also like to thank reviewers Cesar L. Schultz and Graciela
514 Piñeiro for their comments that greatly improved this manuscript. This work was supported by
515 the German Research Foundation (DFG FR 2457/6-1).

516
517

References

519 Araújo DC. 1976. Taxonomia e Relações dos Proganosauria da Bacia do Paraná. *Anais da*
520   *Academia Brasileira de Ciências* 48:91–116.
521 Arthur KE, Boyle MC, Limpus CJ. 2008. Ontogenetic changes in diet and habitat use in green
522   sea turtle (Chelonia mydas) life history. *Marine Ecology Progress Series* 362:303–311.
523   DOI: 10.3354/meps07440.
524 Bastos LPH, Rodrigues R, Pereira E, Bergamaschi S, Alferes CLF, Augland LE, Domeier M,
525   Planke S, Svensen HH. 2021. The birth and demise of the vast epicontinental Permian
526   Irati-Whitehill sea: Evidence from organic geochemistry, geochronology, and
527   paleogeography. *Palaeogeography, Palaeoclimatology, Palaeoecology* 562:110103.
528   DOI: 10.1016/j.palaeo.2020.110103.
529 Bickelmann C, Tsuji LA. 2018. A case study of developmental palaeontology in *Stereosternum*
530   *tumidum* (Mesosauridae, Parareptilia). *Fossil Record* 21:109–118. DOI: 10.5194/fr-21-
531   109-2018.
532 Braun J, Reif W-E. 1985. A survey of aquatic locomotion in fishes and tetrapods. *Neues*
533   *Jahrbuch für Geologie und Paläontologie, Abhandlungen* 169:307–332.

534   Canoville A, Laurin M. 2010. Evolution of humeral microanatomy and lifestyle in amniotes, and
535   some comments on palaeobiological inferences. *Biological Journal of the Linnean*
536   *Society* 100:384–406. DOI: 10.1111/j.1095-8312.2010.01431.x.
537   Carroll RL. 1988. *Vertebrate paleontology and evolution*. New York.
538   Chahud A, Petri S. 2013. The silty shale Taquaral Member of the early Permian Irati Formation
539   (Paraná Basin, Brazil). Paleontology and paleoenvironments. *Swiss Journal of*
540   *Palaeontology* 132:119–128. DOI: 10.1007/s13358-013-0055-1.
541   Cope ED. 1886. A contribution to the vertebrate paleontology of Brazil. *Proceedings of the*
542   *American Philosophical Society* 23:1–21.
543   Dick DG, Schweigert G, Maxwell EE. 2016. Trophic niche ontogeny and palaeoecology of early
544   Toarcian Stenopterygius (Reptilia: Ichthyosauria). *Palaeontology* 59:423–431. DOI:
545   10.1111/pala.12232.
546   Ford DP, Benson RBJ. 2020. The phylogeny of early amniotes and the affinities of Parareptilia
547   and Varanopidae. *Nature Ecology & Evolution* 4:57–65.
548   Gervais P. 1869. Du *Mesosaurus tenuidens*, Reptile fossile de l'Afrique australe. In: *Zoologie et*
549   *paléontologie générales*. Paris: Arthus Bertrand,.
550   Gignac PM, Erickson GM. 2015. Ontogenetic changes in dental form and tooth pressures
551   facilitate developmental niche shifts in American alligators. *Journal of Zoology* 295:132–
552   142. DOI: 10.1111/jzo.12187.
553   Gilabert J. 2001. Seasonal plankton dynamics in a Mediterranean hypersaline coastal lagoon: the
554   Mar Menor. *Journal of Plankton Research* 23:207–218. DOI: 10.1093/plankt/23.2.207.
555   Huxley J. 1932. *Problems of relative growth*. Baltimore: Johns Hopkins University Press.
556   Klein N, Verrière A, Sartorelli H, Wintrich T, Fröbisch J. 2019. Microanatomy and growth of the
557   mesosaurs Stereosternum tumidum and Brazilosaurus sanpauloensis (Reptilia,
558   Parareptilia). *Foss. Rec.* 22:91–110. DOI: 10.5194/fr-22-91-2019.
559   Klingenberg CP. 1998. Heterochrony and allometry: the analysis of evolutionary change in
560   ontogeny. *Biological Reviews* 73:79–123. DOI: https://doi.org/10.1111/j.1469-
561   185X.1997.tb00026.x.
562   Laurin M, Piñeiro G. 2017. A reassessment of the taxonomic position of mesosaurs, and a
563   surprising phylogeny of early amniotes. *Frontiers in Earth Science* 5:88. DOI:
564   10.3389/feart.2017.00088.
565   MacDougall MJ, Modesto SP, Brocklehurst N, Verrière A, Reisz RR, Fröbisch J. 2018.
566   Response: a reassessment of the taxonomic position of Mesosaurs, and a surprising
567   phylogeny of early amniotes. *Frontiers in Earth Science* 6. DOI: 10/gfgxth.
568   MacDougall MJ, Verrière A, Wintrich T, LeBlanc ARH, Fernandez V, Fröbisch J. 2020.
569   Conflicting evidence for the use of caudal autotomy in mesosaurs. *Scientific Reports*
570   10:1–9. DOI: 10.1038/s41598-020-63625-0.
571   MacGregor JH. 1908. On *Mesosaurus brasiliensis* nov. sp. from the Permian of Brazil. In: White
572   IC ed. *Relatório final da Comissão de Estudos das Minas de Carvão de Pedra do Brasil*.
573   Rio de Janeiro: Imprensa Nacional, 301–336.

574   Matos SA, Warren LV, Varejão FG, Assine ML, Simões MG. 2017. Permian endemic bivalves
575   of the "Irati anoxic event", Paraná Basin, Brazil: Taphonomical, paleogeographical and
576   evolutionary implications. *Palaeogeography, Palaeoclimatology, Palaeoecology* 469:18–
577   33. DOI: 10.1016/j.palaeo.2016.12.043.
578   Modesto SP. 1999. Observations on the structure of the Early Permian reptile *Stereosternum
579   tumidum* Cope. *Palaeontologia Africana* 35:7–19.
580   Modesto SP. 2006. The cranial skeleton of the Early Permian aquatic reptile *Mesosaurus
581   tenuidens*: implications for relationships and palaeobiology. *Zoological Journal of the
582   Linnean Society* 146:345–368. DOI: 10.1111/j.1096-3642.2006.00205.x.
583   Modesto SP. 2010. The postcranial skeleton of the aquatic parareptile *Mesosaurus tenuidens*
584   from the Gondwanan Permian. *Journal of Vertebrate Paleontology* 30:1378–1395. DOI:
585   10.1080/02724634.2010.501443.
586   Ng C, Vega CS, Maranhão M da SAS. 2019. Mixed carbonate-siliciclastic microfacies from
587   Permian deposits of Western Gondwana: Evidence of gradual marine to continental
588   transition or episodes of marine transgression? *Sedimentary Geology* 390:62–82. DOI:
589   10.1016/j.sedgeo.2019.07.006.
590   Núñez Demarco P, Ferigolo J, Piñeiro G. 2022. Isometry in mesosaurs: Implications for growth
591   patterns in early amniotes. *Acta Palaeontologica Polonica* 67.
592   Núñez Demarco P, Meneghel M, Laurin M, Piñeiro G. 2018. Was *Mesosaurus* a fully aquatic
593   reptile? *Frontiers in Ecology and Evolution* 6. DOI: 10.3389/fevo.2018.00109.
594   Oelofsen BW, Araújo DC. 1983. Palaeoecological implications of the distribution of mesosaurid
595   reptiles in the Permian Irati Sea (Paraná basin), South America. *Revista Brasileira de
596   Geociências* 13:1–6.
597   Oelofsen BW, Araújo DC. 1987. *Mesosaurus tenuidens* and *Stereosternum tumidum* from the
598   Permian Gondwana of both southern Africa and South America. *South African Journal of
599   Science* 83:370–372.
600   Parker RH. 1959. Macro-invertebrate assemblages of Central Texas coastal bays and Laguna
601   Madre. *AAPG Bulletin* 43:2100–2166. DOI: 10.1306/0BDA5EA3-16BD-11D7-
602   8645000102C1865D.
603   Piñeiro G, Ferigolo J, Meneghel M, Laurin M. 2012a. The oldest known amniotic embryos
604   suggest viviparity in mesosaurs. *Historical Biology* 24:620–630. DOI:
605   10.1080/08912963.2012.662230.
606   Piñeiro G, Ferigolo J, Mones A, Núñez Demarco P. 2021. Mesosaur taxonomy reappraisal: are
607   *Stereosternum* and *Brazilosaurus* valid taxa? *Revista Brasileira de Paleontologia*
608   24:205–235. DOI: 10.4072/rbp.2021.3.04.
609   Piñeiro G, Núñez Demarco P, Meneghel MD. 2016. The ontogenetic transformation of the
610   mesosaurid tarsus: a contribution to the origin of the primitive amniotic astragalus. *PeerJ*
611   4:e2036.

612 Piñeiro G, Ramos A, Goso C, Scarabino F, Laurin M. 2012b. Unusual environmental conditions
613   preserve a Permian mesosaur-bearing Konservat-Lagerstätte from Uruguay. *Acta*
614   *Palaeontologica Polonica* 57:299–318. DOI: 10.4202/app.2010.0113.
615 Pretto F, Cabreira SF, Schultz CL. 2012. Tooth microstructure of the Early Permian aquatic
616   predator *Stereosternum tumidum* and paleobiological implications. *Acta Palaeontologica*
617   *Polonica* 59:125–133. DOI: 10.4202/app.2011.0121.
618 R. Core Team. 2021. *R: a language and environment for statistical computing*. Vienna, Austria:
619   R Foundation for Statistical Computing.
620 Ramos A. 2015. La dieta de los Mesosauridae (Amniota: Proganosauria) del Pérmico temprano
621   de Uruguay. BS Thesis Thesis. Montevideo: Universidad de la República.
622 de Ricqlès A. 1974. Recherches paléohistologiques sur les os longs des tétrapodes V.
623   Cotylosaures et mésosaures. *Annales de Paléontologie* 60:171–216.
624 Rossmann T. 2000. Studien an Mesosauriern (Amniota inc. sed.: Mesosauridae): 2. Neue
625   Erkenntnisse zur Anatomie, mit Berücksichtigung der Taxonomie von *Mesosaurus*
626   *pleurogaster* (Seeley). In: Storch G, Weddige K eds. *Advances in Vertebrate*
627   *Palaeontology*. Frankfurt am Main: Schweizerbartische Verlagsbuchhandlung, 13–28.
628 Rossmann T. 2002. Studien an Mesosauriern (Amniota inc. sed., Mesosauridae): 3. Neue
629   Aspekte zur Anatomie, Erhaltung und Paläoökologie aufgrund der Exemplare im
630   Paläontologischen Institut der Universität Zürich. *Neues Jahrbuch für Geologie und*
631   *Paläontologie, Abhandlungen*:197–221.
632 Rossmann T, Maisch MW. 1999. Das Mesosaurier-Material in der Bayerischen Staatssammlung
633   für Paläontologie und Historische Geologie: Übersicht und neue Erkenntnisse.
634   *Mitteilungen der Bayerischen Staatssammlung für Paläontologie und historische*
635   *Geologie.* 36:69–81.
636 Shikama T, Ozaki H. 1966. On a reptilian skeleton from the Paleozoic formation of San Paulo,
637   Brazil. *Transactions and Proceedings of the Paleontological Society of Japan* 64:351–
638   358.
639 da Silva RC, Sedor FA. 2017. Mesosaurid swim traces. *Frontiers in Ecology and Evolution* 5.
640   DOI: 10.3389/fevo.2017.00022.
641 Silva RR, Ferigolo J, Bajdek P, Piñeiro G. 2017. The feeding habits of Mesosauridae. *Frontiers*
642   *in Earth Science* 5. DOI: 10.3389/feart.2017.00023.
643 Soares MB. 2003. A taphonomic model for the Mesosauride assemblage of the Irati Formation
644   (Paraná Basin, Brazil). *Geologica Acta* 1:349–361. DOI: 10.1344/105.000001621.
645 Tanner R, Glenn EP, Moore D. 1999. Food Chain Organisms in Hypersaline, Industrial
646   Evaporation Ponds. *Water Environment Research* 71:494–505. DOI:
647   10.2175/106143097X122149.
648 Verrière A, Fröbisch NB, Fröbisch J. 2021. *Regionalization, constraints, and the ancestral*
649   *ossification patterns in the vertebral column of amniotes*. DOI:
650   10.1101/2021.09.23.461462.

651   Villamil J, Núñez Demarco P, Meneghel M, Blanco RE, Jones W, Rinderknecht A, Laurin M,
652   Piñeiro G. 2015. Optimal swimming speed estimates in the Early Permian mesosaurid
653   *Mesosaurus tenuidens* (Gervais 1865) from Uruguay. *Historical Biology*:1–9. DOI:
654   10/gfgxtm.
655   Wang S, Stiegler J, Amiot R, Wang X, Du G, Clark JM, Xu X. 2017. Extreme ontogenetic
656   changes in a ceratosaurian theropod. *Current Biology* 27:144–148. DOI:
657   10.1016/j.cub.2016.10.043.
658   Wiman C. 1925. Zur Kenntnis der Mesosaurier. In: Gorjanović-Krambergeriana X ed.
659   *Spomenica u počast prof. dr. Gorjanović-Krambergeru*. Zagreb, 411–423.
660   Xavier PLA, Silva AF, Soares MB, Horn BLD, Schultz CL. 2018. Sequence stratigraphy control
661   on fossil occurrence and concentration in the epeiric mixed carbonate-siliciclastic ramp
662   of the Early Permian Irati Formation of southern Brazil. *Journal of South American Earth*
663   *Sciences*. DOI: 10.1016/j.jsames.2018.08.014.
664

Figure 1

Comparison of morphologies in juvenile and adult mesosaurs.

Scale bars equal 20 mm. **A.** Side-by-side comparison of a juvenile (BSPG 1979 I 37, on the left) and an adult *"Stereosternum tumidum"* (MB.R.5605, on the right) showing the ontogenetically changing proportions. **B.** Close-up of the skull of adult *Mesosaurus tenuidens* NRM PZ R 207c showing the characteristic needle-like teeth of mesosaurs. **C.** Close-up of juvenile *"Stereosternum tumidum"* GP/2E 9233 with arrows showing the shorter teeth of immature individuals.
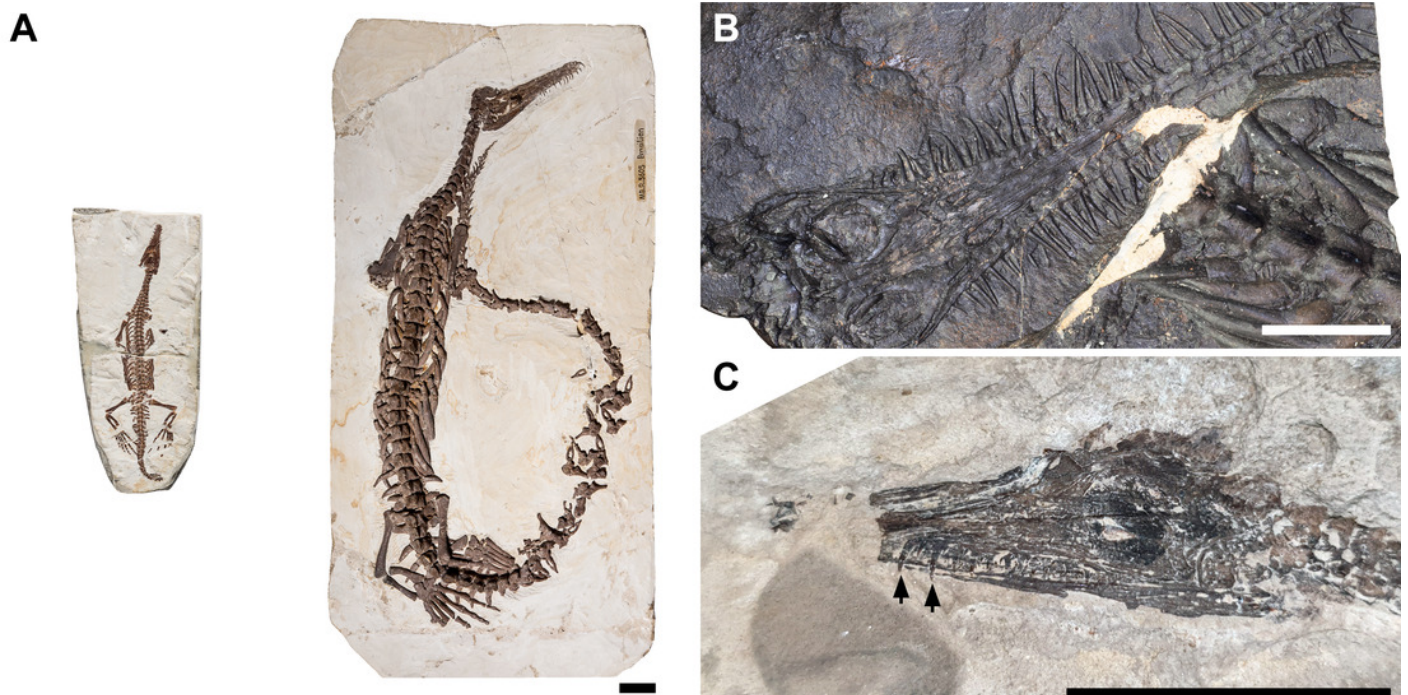
Figure 2

Measurement/size ratios in function of size under the three-species hypothesis.
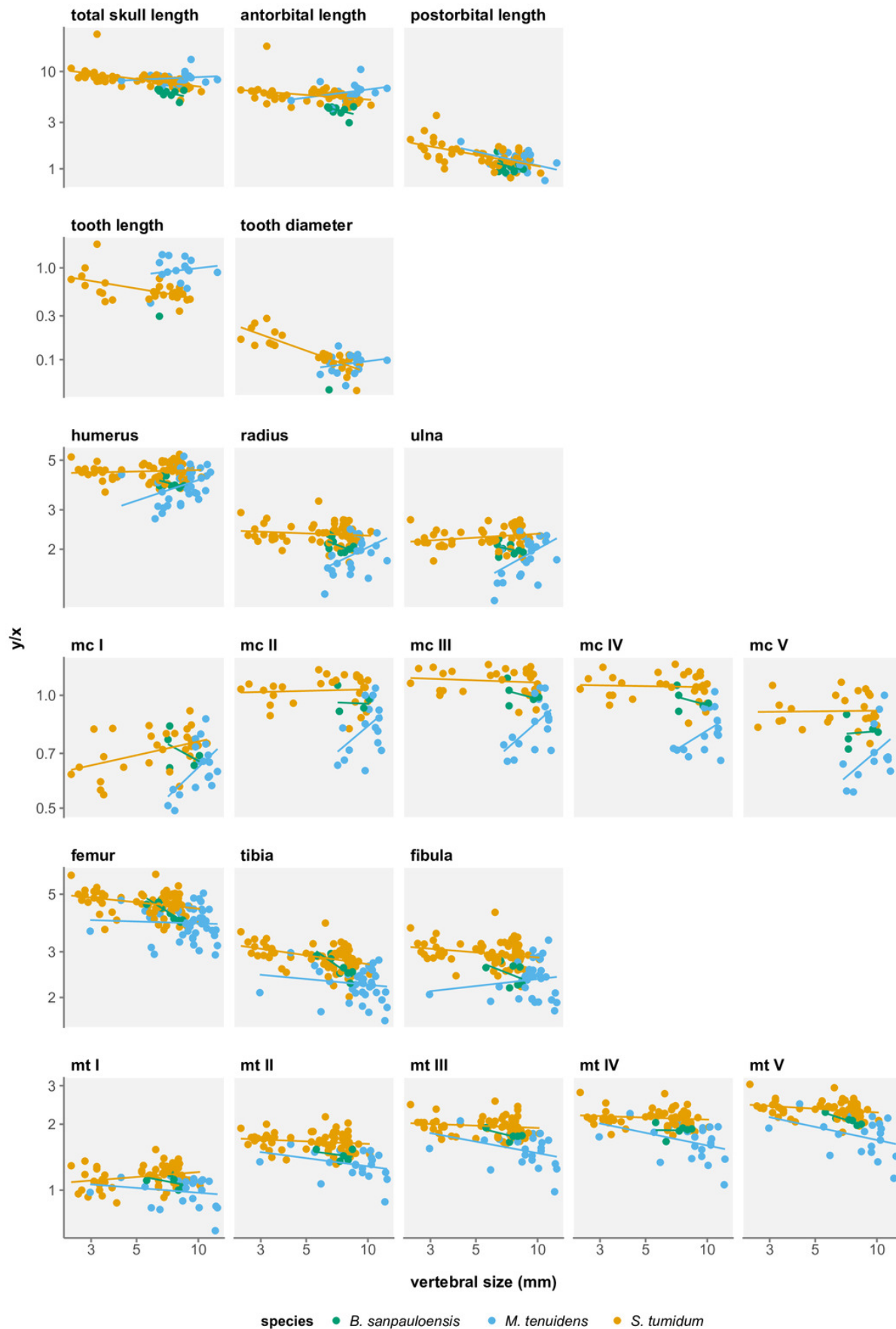
Logged scale.

Figure 3

Comparison of skull measurements/total skull length ratios in function of total skull length under the three-species and the single-species hypothesis.
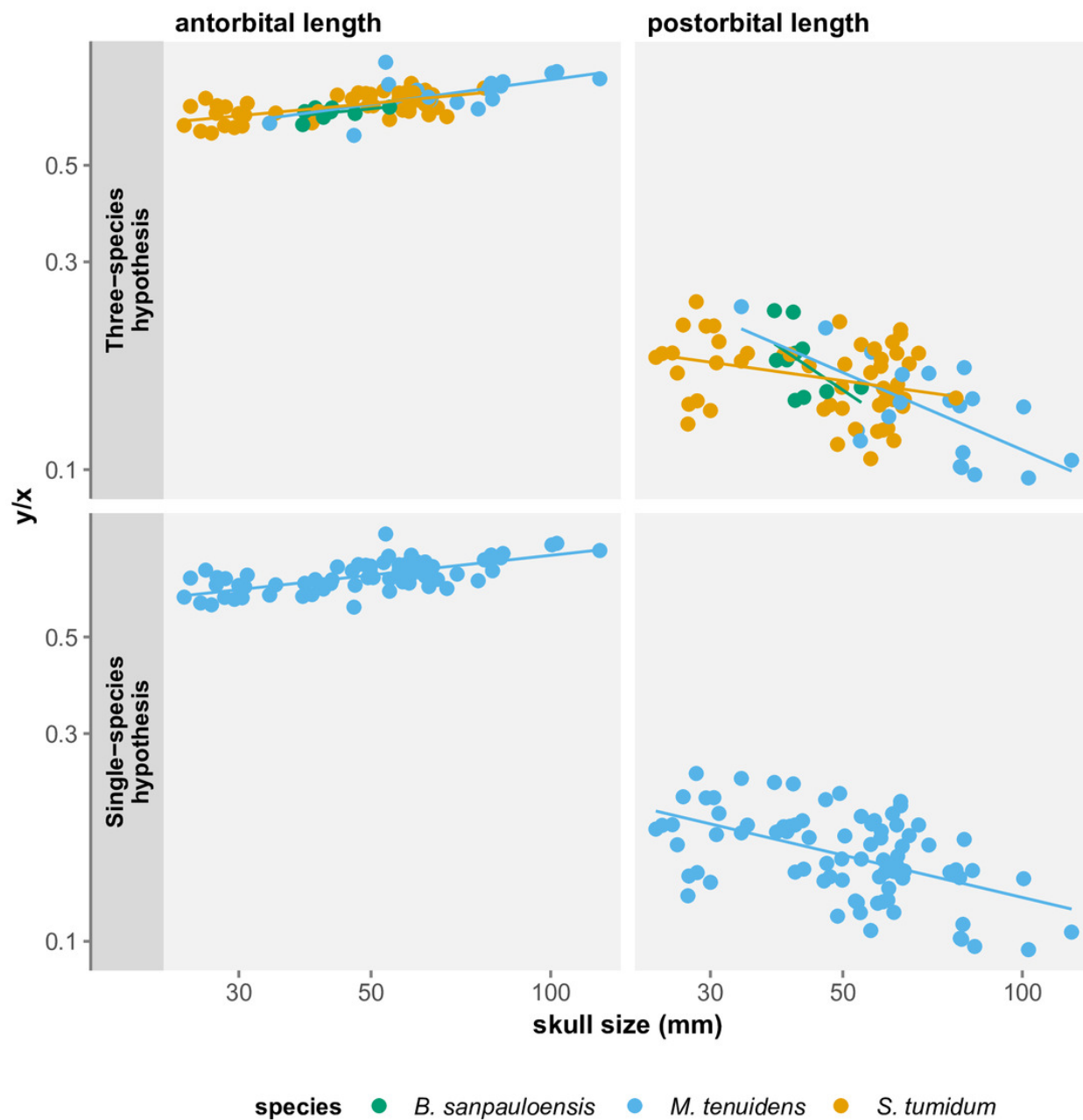
Logged scale.

Figure 4

Comparison of tooth measurements/total skull length ratios in function of total skull length under the three-species and the single-species hypothesis.
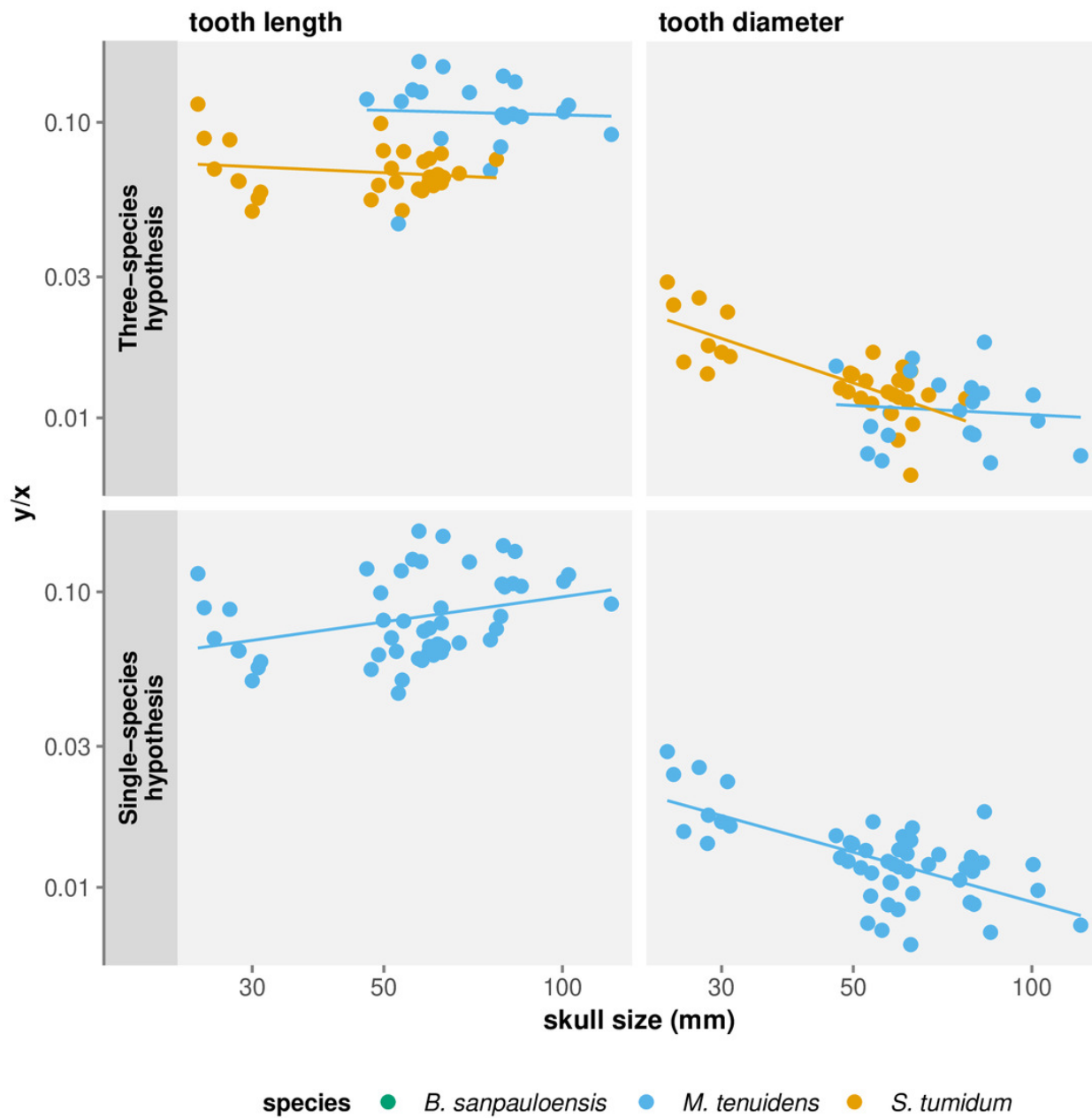
Logged scale.

Figure 5

Measurement/size ratios in function of size under the single-species hypothesis.

Logged scale.

total skull length   antorbital length   postorbital length

tooth length   tooth diameter

humerus   radius   ulna

y/x

mc I   mc II   mc III   mc IV   mc V

femur   tibia   fibula

mt I   mt II   mt III   mt IV   mt V
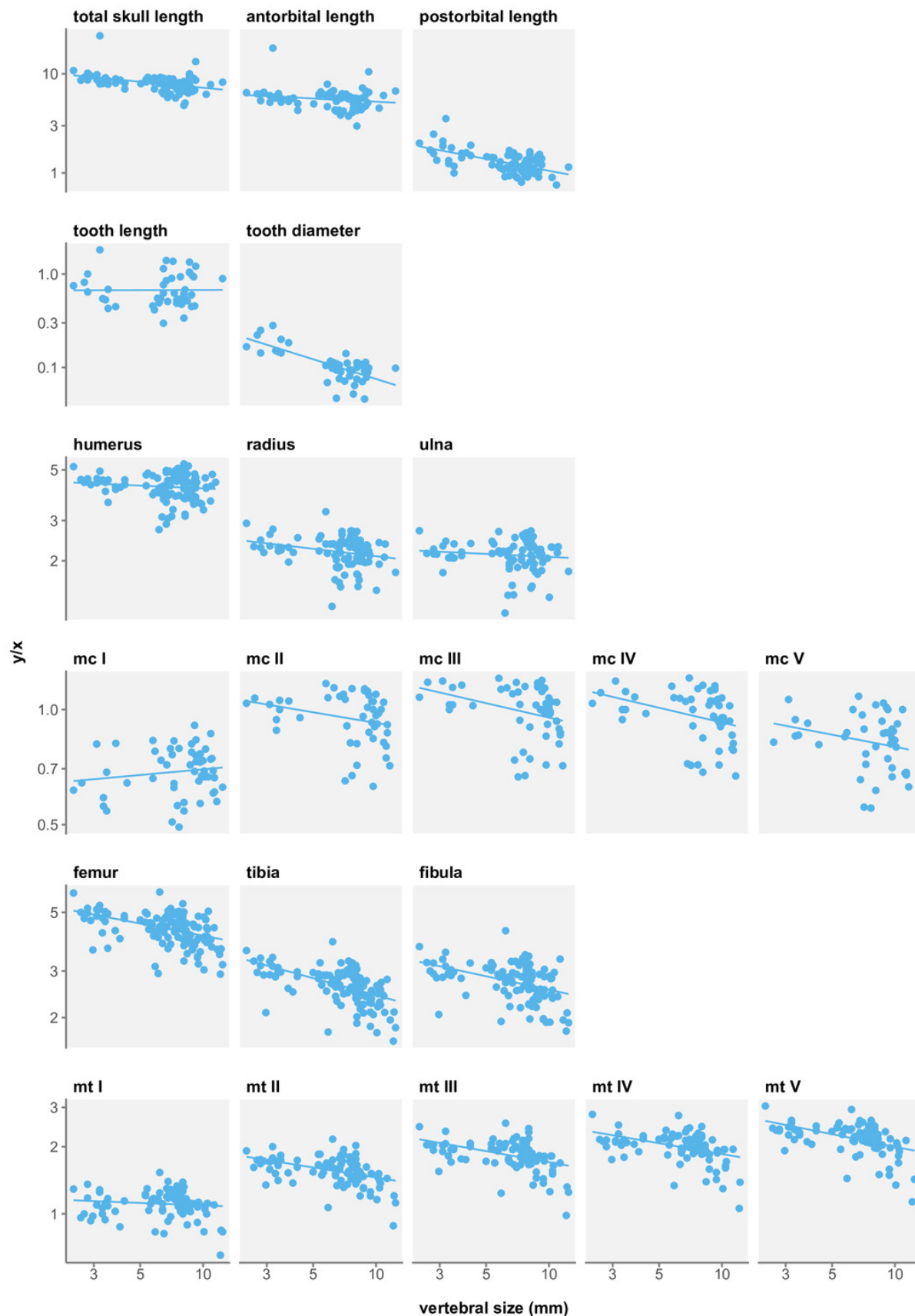
vertebral size (mm)

Figure 6

Size distribution of vertebral size per geological facies under the single-species hypothesis

Facies are organized top to bottom along a gradient of depth as depicted to the right, and following the deposition models from Xavier et al. (2018) and Ng et al. (2019). The energy level gradient on the right corresponds to grain size in the sediment. There is a clear overrepresentation of juveniles in limestone, as well as an overrepresentation of large specimens in black shale.

![Histograms of vertebral size (mm) for five lithologies — limestone (n = 61), calcarenite (n = 36), siltstone (n = 30), mudstone (n = 12), and black shale (n = 69) — with depth and energy level gradient scales on the right.]
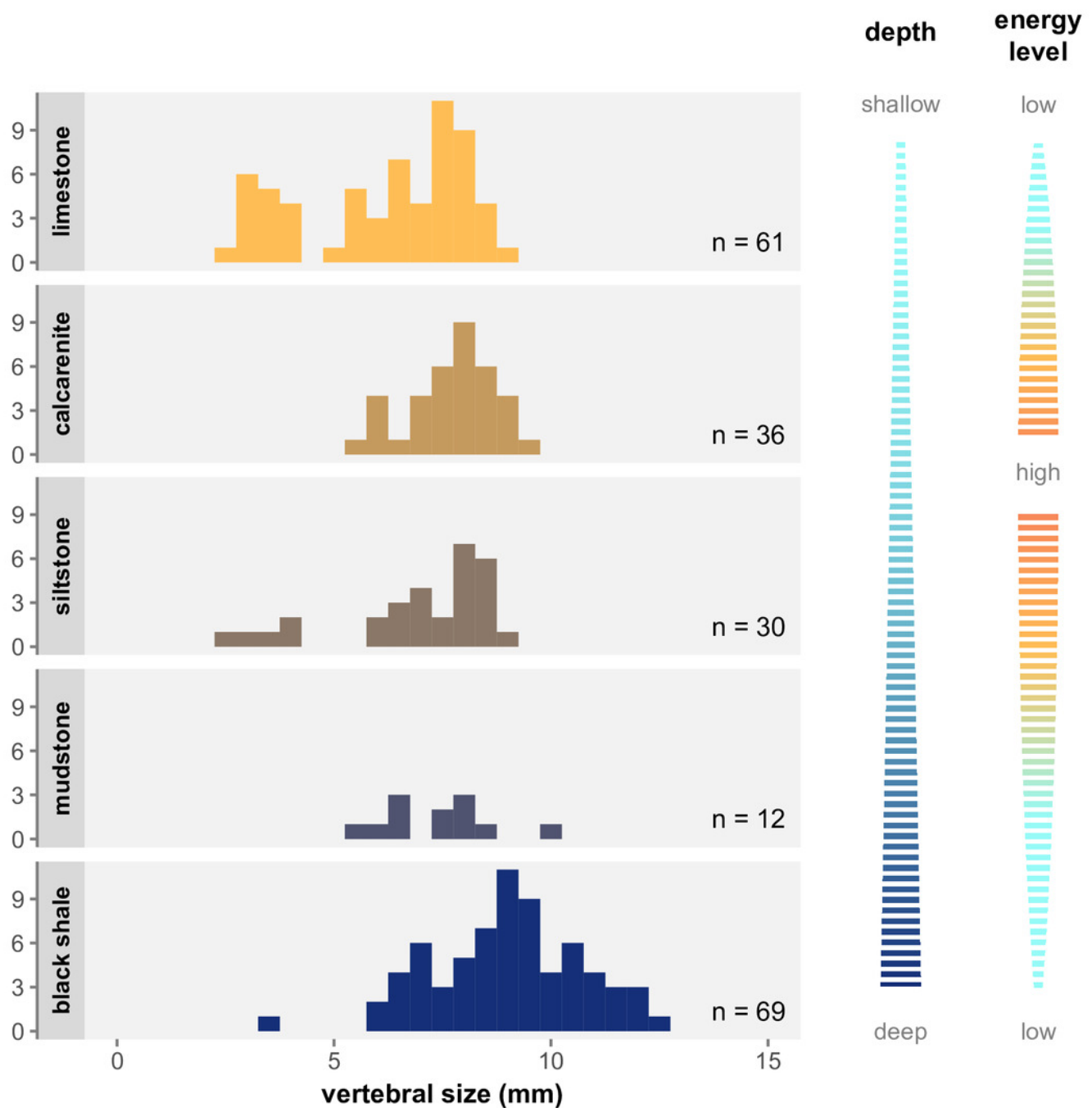
Figure 7

Histogram of average vertebral size under the three-species hypothesis.

Small/juvenile specimens are notably overrepresented in the "*S. tumidum*" group, whereas large individuals are only represented in the *M. tenuidens* group.
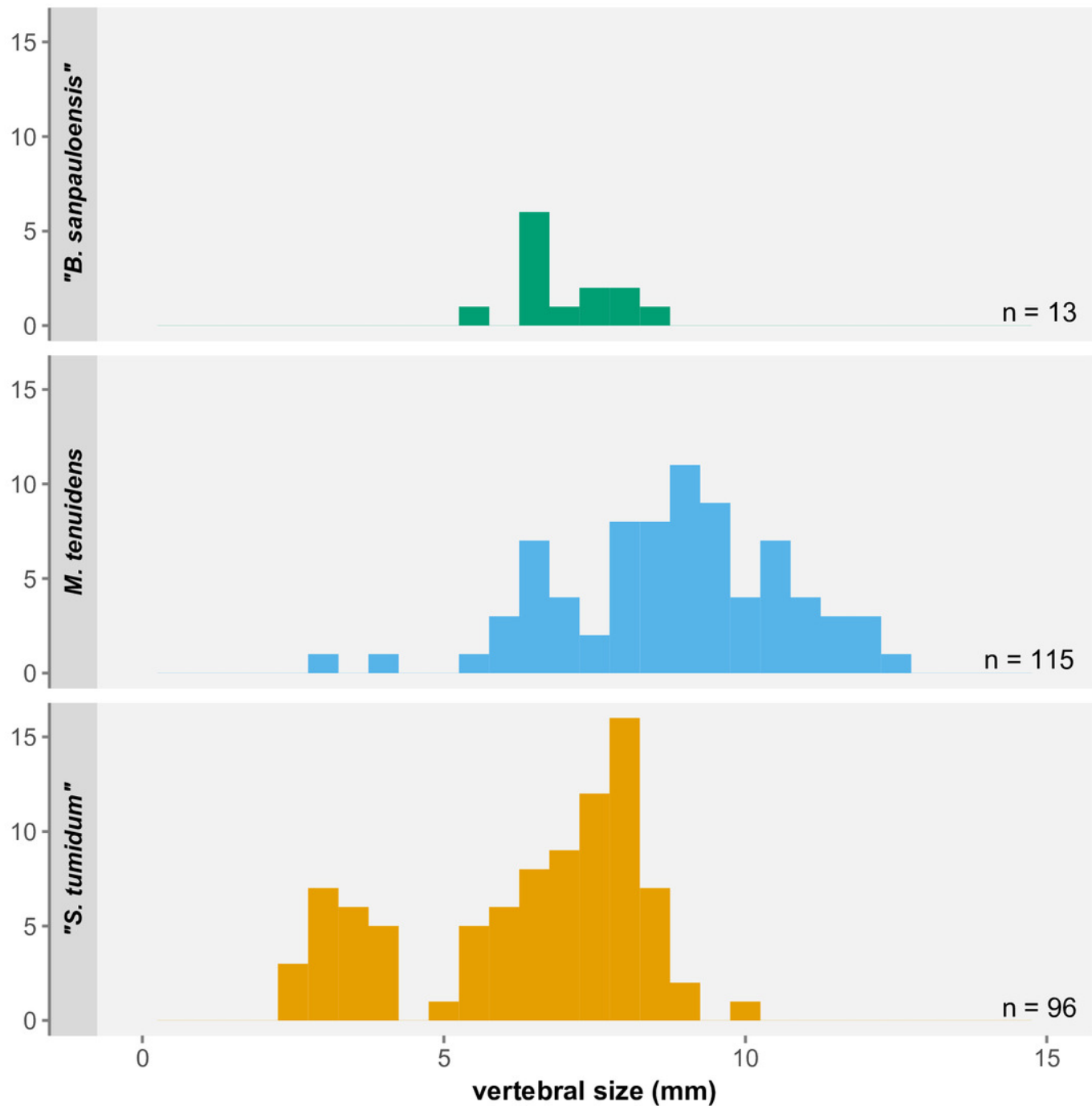
Allometry coefficient of logged size ratios for teeth and skull measurements.

1   **Table 1**. Allometry coefficient of logged size ratios for teeth and skull measurements.

	Allometry coefficient β	SE	t-value	p-value
"B. sanpauloensis"				
tooth length	-	-	-	-
tooth diameter	-	-	-	-
skull total length	−0.462	0.290	−1.596	0.149
skull antorbital length	−0.509	0.362	−1.405	0.198
skull postorbital length	−0.586	0.491	−1.193	0.267
M. tenuidens				
tooth length	0.286	0.417	0.685	0.504
tooth diameter	0.466	0.338	1.380	0.188
skull total length	0.094	0.140	0.268	0.792
skull antorbital length	0.204	0.160	1.279	0.222
skull postorbital length	**−0.511**	**0.275**	**−2.308**	**0.037**
"S." tumidum				
tooth length	**−0.381**	**0.115**	**−3.310**	**0.003**
tooth diameter	**−0.787**	**0.096**	**−8.179**	**< 0.001**
skull total length	**−0.256**	**0.050**	**−5.131**	**< 0.001**
skull antorbital length	**−0.177**	**0.064**	**−2.770**	**0.008**
skull postorbital length	**−0.376**	**0.074**	**−5.076**	**< 0.001**
Single-species hypothesis				
tooth length	0.029	0.149	0.191	0.849
tooth diameter	−0.653	0.106	−6.190	**< 0.001**
skull total length	−0.203	0.050	−4.090	**< 0.001**
skull antorbital length	−0.122	0.066	−1.835	0.070
skull postorbital length	**−0.392**	**0.062**	**−6.296**	**< 0.001**

Allometry coefficients of logged tooth and skull measurements with respect to total skull length.

1 **Table 2.** Allometry coefficients of logged tooth and skull measurements with respect to total
2 skull length.

	Allometry coefficient β	SE	t-value	p-value
"B. sanpauloensis"				
tooth length	-	-	-	-
tooth diameter	-	-	-	-
skull antorbital length	0.134	0.086	1.563	0.157
skull postorbital length	−0.925	0.522	−1.771	0.114
M. tenuidens				
tooth length	−0.051	0.276	−0.186	0.855
tooth diameter	−0.103	0.260	−0.398	0.696
skull antorbital length	0.187	0.058	3.206	**0.005**
skull postorbital length	−0.590	0.156	−3.785	**0.001**
"S. tumidum"				
tooth length	−0.091	0.097	−0.936	0.357
tooth diameter	−0.678	0.107	−6.336	**< 0.001**
skull antorbital length	0.121	0.021	5.761	**< 0.001**
skull postorbital length	−0.172	0.076	−2.249	**0.029**
Single-species hypothesis				
tooth length	0.282	0.115	2.456	**0.018**
tooth diameter	−0.558	0.092	−6.082	**< 0.001**
skull antorbital length	0.147	0.017	8.506	**< 0.001**
skull postorbital length	−0.315	0.059	−5.314	**< 0.001**

Allometry coefficient of logged size ratios for long bone lengths.

A. *"B. sanpauloensis"*. **B.** *M. tenuidens.* **C.** "*S.* tumidum" **D.** Single–species hypothesis

1 **Table 3**. Allometry coefficient of logged size ratios for long bone lengths.
2 **A.** "*B. sanpauloensis*"

	Allometry coefficient *β*	SE	t-value	p-value
humerus	−0.044	0.033	−1.321	0.189
radius	−0.081	0.054	−1.497	0.137
ulna	−0.083	0.057	−1.449	0.151
mc I	0.062	0.058	1.078	0.285
mc II	−0.122	0.062	−1.988	0.052
mc III	−0.159	0.063	−2.509	0.015
mc IV	−0.173	0.063	−2.728	0.009
mc V	−0.146	0.081	−1.809	0.077
anterior autopod	0.050	0.212	0.236	0.852
femur	−0.154	0.030	−5.078	**< 0.001**
tibia	−0.212	0.035	−6.119	**< 0.001**
fibula	−0.167	0.039	−4.268	**< 0.001**
mt I	−0.026	0.036	−0.709	0.480
mt II	−0.142	0.035	−4.068	**< 0.001**
mt III	−0.163	0.040	−4.108	**< 0.001**
mt IV	−0.157	0.039	−4.042	**< 0.001**
mt V	−0.185	0.040	−4.630	**< 0.001**
posterior autopod	-	-	-	-

4 **B.** *M. tenuidens*

	Allometry coefficient *β*	SE	t-value	p-value
humerus	0.308	0.125	2.473	**0.018**
radius	0.445	0.171	2.599	**0.016**
ulna	0.515	0.199	2.588	**0.016**
mc I	0.646	0.244	2.650	**0.017**
mc II	0.569	0.282	2.018	0.062
mc III	0.590	0.218	2.713	**0.016**
mc IV	0.417	0.217	1.923	0.077
mc V	0.573	0.308	1.859	0.090
anterior autopod	0.527	0.607	0.867	0.450
Femur	−0.024	0.077	−0.31	0.758
Tibia	−0.074	0.077	−0.952	0.347
Fibula	0.089	0.112	0.799	0.431
mt I	−0.073	0.09	−0.812	0.425
mt II	−0.124	0.082	−1.524	0.143
mt III	−0.175	0.096	−1.828	0.082
mt IV	−0.192	0.105	−1.816	0.084
mt V	−0.199	0.115	−1.728	0.101
posterior autopod	−0.122	0.053	−2.293	0.262

7   **C.** "*S. tumidum*"

	Allometry coefficient β	SE	t-value	p-value
humerus	0.021	0.027	0.771	0.444
radius	−0.034	0.036	−0.936	0.353
ulna	0.057	0.034	1.698	0.095
mc I	0.150	0.056	2.683	**0.012**
mc II	0.017	0.045	0.366	0.717
mc III	−0.024	0.039	−0.616	0.543
mc IV	−0.012	0.041	−0.279	0.782
mc V	0.007	0.058	0.124	0.902
anterior autopod	−0.025	0.066	−0.370	0.716
femur	−0.081	0.029	−2.779	**0.007**
tibia	−0.113	0.03	−3.773	**< 0.001**
fibula	−0.065	0.034	−1.875	0.065
mt I	0.074	0.034	2.173	**0.033**
mt II	−0.038	0.029	−1.304	0.197
mt III	−0.035	0.031	−1.114	0.269
mt IV	−0.031	0.028	−1.089	0.280
mt V	−0.056	0.027	−2.069	**0.043**
posterior autopod	−0.140	0.061	−2.310	**0.028**

9   **D.** Single–species hypothesis

Single species hypothesis	Allometry coefficient β	SE	t-value	p-value
humerus	−0.041	0.035	−1.184	0.239
radius	−0.109	0.043	−2.502	**0.014**
ulna	−0.044	0.046	−0.949	0.346
mc I	0.061	0.057	1.074	0.288
mc II	−0.113	0.062	−1.831	0.073
mc III	−0.154	0.064	−2.411	**0.020**
mc IV	−0.157	0.062	−2.522	**0.015**
mc V	−0.130	0.082	−1.589	0.120
anterior autopod	−0.120	0093	−1.281	0.212
femur	−0.153	0.029	−5.303	**< 0.001**
tibia	−0.215	0.031	−6.875	**< 0.001**
fibula	−0.170	0.037	−4.6	**< 0.001**
mt I	−0.037	0.035	−1.06	0.292
mt II	−0.150	0.034	−4.47	**< 0.001**
mt III	−0.166	0.038	−4.405	**< 0.001**
mt IV	−0.161	0.038	−4.247	**< 0.001**
mt V	−0.187	0.039	−4.774	**< 0.001**
posterior autopod	−0.152	0.053	−2.863	**0.007**

ANOVA results for the effect of species on measurements

1   **Table 4.** ANOVA results for the effect of species on measurements

	df	F	p-value
total skull length	2	13,087	**0,000**
antorbital length	2	11,774	**0,000**
postorbital length	2	4,576	**0,013**
tooth length	1	59,118	**0,000**
tooth diameter	1	2,922	0,094
humerus	2	3,362	**0,038**
radius	2	1,374	0,258
ulna	2	1,923	0,152
mc I	2	2,620	0,082
mc II	2	0,926	0,403
mc III	2	0,445	0,644
mc IV	2	0,380	0,686
mc V	2	0,088	0,916
femur	2	6,282	**0,002**
tibia	2	3,827	**0,025**
fibula	2	4,507	**0,013**
mt I	2	2,912	0,059
mt II	2	1,575	0,213
mt III	2	1,058	0,351
mt IV	2	0,792	0,456
mt V	2	0,501	0,608